



電子 507

# **Fabrication and Characterization of III-Nitride Semiconductor Nanocavity Light Emitters**

(III 族窒化物半導体微小共振器型光源の  
作製と評価に関する研究)

A Thesis Presented to  
the Graduate School of the University of Tokyo  
in Partial Fulfillment of the Requirements  
for the Degree of Doctor of Philosophy  
in Electronic Engineering

by

**Munetaka Arita**

December, 2006

# Preface

This thesis presents a part of the research carried out at Research Center for Advanced Science and technology (RCAST), and Institute of Industrial Science (IIS) of the University of Tokyo under the supervision of Professor Yasuhiko Arakawa, while the author was a graduate student in the Department of Electronic Engineering at the University of Tokyo from October 2000 to March 2007.

In this thesis, fabrication processes and optical characteristics of III-Nitride semiconductor nanocavity light emitters are described.

December 15, 2006

Munetaka Arita



# Acknowledgements

The author would like to express his sincere gratitude to his dissertation supervisor, Professor Yasuhiko Arakawa, Research Center of Advanced Science and Technology, The University of Tokyo, for his continuous encouragement and support. His endless and respectable enthusiasm for the scientific works and generous guidance have been invaluable. Without them, the author could have never achieved the goal.

The author would like to thank the Electronic Engineering faculty at The University of Tokyo for their assistance of my research. In particular, he would like to thank the members of his dissertation committee: Professor Hiroyuki Sakaki, Professor Kazuhiko Hirakawa, Professor Yoshiaki Nakano, Professor Masaaki Tanaka, Professor Takao Someya, and Professor Satoshi Iwamoto.

The author would like to express his sincere gratitude to Professor Takao Someya, Department of Engineering, The University of Tokyo, for his technical guidance. Without his outstanding insight and knowledge as well as continuous effort, the initial stage of this research could not be established.

The author would also like to acknowledge Professor Satoshi Iwamoto, Research Center of Advanced Science and Technology, The University of Tokyo, for fruitful discussions and helpful supports on the nitride photonic crystal project. A lot of computer simulations were owed to him. Draft of technological literatures were sincerely reviewed and commented by him.

A lot of this work was supported by various people. The author would like to acknowledge Mr. Masao Nishioka, Assistant of Institute of Industrial Science, The University of Tokyo, for his technical support especially with the MOCVD system. The author also would like to thank Professor Katsuyuki Hoshino, Yamaguchi University, for his assistance dedicated to maintenance of the MOCVD system, as well as useful discussion on nitride semiconductor growth. Also thanks to Drs. Naoya Okamoto, Fujitsu Laboratory, and Masahiro Nomura for their technical assistances. The MOCVD system used in this research is so delicate that we must spend many hours to keep the

reactor clean enough to grow high quality nitrides. The author would like to thank Dr. Koichi Tachibana, Toshiba and Mr. Makoto Miyamura, NEC, for their technical supports and guidance with which the author had been able to handle the system.

The author would like to thank Mr. Satomi Ishida, Assistant of Research Center for Advanced Science and Technology, The University of Tokyo, for his great skills with which he could fabricate fine patterns by electron-beam lithography. The author owes plenty part of photolithography to Dr. Masatoshi Kitamura, who kindly helped him to fabricate masks.

Optical measurements were collaborative works with Drs. Satoshi Kako, and Toshihiro Nakaoka, whom the author would like to thank very much. He also thanks Dr. Seiji Nagahara and Mr. Takeshi Kawano for their technical support on photoluminescence measurements.

The author would like to acknowledge Ms. Ning Li for her excellent contribution in fabrication of nitride photonic crystals. Especially, dry etching procedures for patterning fine features in nitride materials are completely owed to her. Initial stage of the research was not established without her continuous efforts.

Appreciation is also extended to Mr. Aniwat Tандаechnurat for his great help with the theoretical analyses. Without the support, the author would not have gotten any valuable information on the nature of photonic crystals.

The author would like to thank all his colleagues, as well as all of our laboratory's secretaries.

The author would like to acknowledge financial support from the Research Fellowships for Young Scientists provided by Japan Society for the Promotion of Science as well as additional support from the 21st Century Center of Excellence in Electrical Engineering and Electronics for the Active and Creative World, The University of Tokyo.

This research was partly supported by the Focused Research and Development Project for the Realization of the World's Most Advanced IT Nation, IT Program, Ministry of Education, Culture, Sports, Science and Technology (MEXT), Japan.

This work was also supported by Special Coordination Funds for Promoting Science and technology, MEXT, Japan.

Finally, the author would like to acknowledge supports from his family, especially the kindest, loving one from his wife, Kaoru. Without their supports, encouragements, and understandings, this work could never be accomplished.

# Abstract

This thesis describes III-nitride semiconductor nanocavity light emitters from the viewpoints of both fabrication technologies and their optical characteristics. Performances of conventional nitride light emitters such as spectral purity, modulation bandwidth, and directionality can be greatly improved by incorporating vertical microcavities. III-nitride photonic crystal nanocavities with embedded quantum dots deserve consideration as possible candidates of high-efficiency single-photon emitters operating at moderately high temperature. In order to realize such highly-engineered III-nitride nanocavity light emitters, progresses have been made in fabrication of two different structures: vertical microcavity surface-emitting diodes and two-dimensional photonic crystal nanocavities.

In Chapter 2, Basic principles of crystal growth of III-nitride semiconductors by metalorganic chemical vapor deposition (MOCVD) are presented. Details on experimental setups for the growth as well as fundamentals on MOCVD growth of nitride quantum dots are also given. Special efforts are made to improve crystal quality of thin AlN layers requisite to construct photonic crystal slab structure. Utilizing alternate supply of source gases, thin AlN layer with sufficient quality is able to be grown. GaN QDs are grown on the thin AlN layer and characterized.

In Chapter 3, MOCVD growth of electrically conductive AlGaN/GaN DBRs is discussed. Structural, optical and electrical properties of the DBRs are studied systematically. From Si doping concentration dependence of structural and optical properties of n-DBRs, it can be concluded that reasonable reflectivity can be maintained with uniform carrier concentration profile of  $1 \times 10^{18} \text{ cm}^{-3}$ . The author shows that the carrier concentration in n-AlGaN layers can be increased up to  $3 \times 10^{18} \text{ cm}^{-3}$  while that of n-GaN is kept at constant value,  $1 \times 10^{18} \text{ cm}^{-3}$ , without further degradation of optical properties. Using such modulated doping profiles, electrical properties of the n-DBRs can be improved. As a result, it is possible to obtain near 99 % reflectivity in electrically conductive n-type nitride DBRs. Further improvement in both structural and electrical characteristics can be achieved

by introducing n-AlGaIn/n-GaN short-period superlattice into the n-DBRs.

In Chapter 4, Developments of fabrication processes for nitride vertical microcavity light emitting devices are presented. Because at least one of cavity mirrors is made by insulating materials in practical device structures, it is reasonable to utilize transparent intracavity contact to overcome design issues concerning efficient hole current injection. For this purpose, indium tin oxide (ITO) is used in this study. Rapid thermal annealing of sputtered ITO films under nitrogen ambient can improve both electrical and optical properties of the films. To improve process yield in photolithographic liftoff, new double-layer resist technique is developed. Undercut resist profile favorable for liftoff as well as good adhesion onto nitride (and ITO) surface is available with this new method. Substrate preparation method to prevent thick AlGaIn/GaN DBR to crack is also established.

In Chapter 5, the author describes fabrication and characterization of InGaIn vertical microcavity LEDs. Magnetron-sputtered, transparent ITO film is employed as a p-contact. After the LED mesas is defined by Cl<sub>2</sub>-based plasma etching, a 10.5 pairs of SiO<sub>2</sub>/ZrO<sub>2</sub> top mirror is evaporated and wet-etched, followed by formation of an Al n-contact. EL spectra of these LEDs have reduced linewidth, exhibiting clear effects of microcavity. The angle dependence of EL reveals blue shift of main mode due to DBR resonance. Furthermore, directionality of the microcavity LED is dramatically improved to half angle of around 10 degree, compared to that of conventional one. The results are promising for developing blue/ultraviolet VCSELs and high performance LEDs, as well as electrically-pumped single photon emitters.

In Chapter 6, Developments of fabrication processes for AlN photonic crystal nanocavities are described. Preliminary calculations reveal technological requirements for the fabrication. In addition to the requirement for fine patterns as small as 150-nm-period, the substrate must be removed in order to obtain sufficient optical confinement in the nanocavities. To this end, photoelectrochemical etching is employed to fabricate AlN photonic crystal nanocavities. Due to accumulated photogenerated holes, lateral etching of 6H-SiC substrate occurs just below the AlN/SiC interface, and partial lift-off of AlN epitaxial layer results in a convex-shaped air-bridge structure.

In Chapter 7, experimental results are given on optical characterization of AlN photonic crystal nanocavities with GaN quantum dots. Microscopic photoluminescence measurements are performed to investigate the optical properties of the nanocavities. For the lowest-order cavity mode of a 150-nm-period nanocavity with seven missing holes, luminescence linewidth of 0.16 nm

corresponding to the  $Q$ -factor of more than 2,400, which is the highest  $Q$  for nitride-based PC nanocavities ever reported, was obtained. Discussions on the results are also presented.

In Chapter 8, summary of this thesis is presented. Future prospects of this research is also given.

In summary, fabrication technologies of III-nitride semiconductor nanocavity light emitters are newly developed and fundamental characteristics of the structures are demonstrated.

The author believes these experimental results facilitate further development of nitride-based ultraviolet quantum optoelectronic devices such as single photon emitters.



# Contents

<b>Preface</b>	i
<b>Acknowledgements</b>	iii
<b>Abstract</b>	v
<b>Contents</b>	ix
<b>Chapter 1 Introduction</b>	1
1.1 Background and Main Object of This Research	1
1.2 Outline of This Thesis	6
<b>Chapter 2 Crystal Growth of III-Nitride Semiconductors by Metalorganic Chemical Vapor Deposition</b>	9
2.1 Introduction	9
2.2 Principles of Crystal Growth of III-Nitride Semiconductors by Metalorganic Chemical Vapor Deposition	10
2.3 General Growth Conditions for III-Nitride Vertical Microcavity Light Emitting Devices	13
2.4 General Growth Conditions for GaN/AlN Quantum Dots	16
2.5 Summary	22
<b>Chapter 3 MOCVD Growth of Electrically Conductive AlGaIn/GaN Distributed Bragg Reflectors with High Reflectivity</b>	23
3.1 Introduction	23
3.2 Growth of III-Nitride Distributed Bragg Reflectors by Atmospheric Pressure Metalorganic Chemical Vapor Deposition	24
3.3 Si Doping into AlGaIn/GaN Distributed Bragg Reflectors	25
3.3.1 Doping Concentration Dependence	26

3.3.2	Total Thickness Dependence	26
3.3.3	Improvement of Electrical Properties by Intense Doping into AlGaN	28
3.4	Introduction of AlGaN/GaN Superlattices	29
3.4.1	Effects of AlGaN/GaN Superlattices on Strain	29
3.4.2	Characterization of Superlattice DBRs	31
3.5	High Reflectivity III-Nitride DBRs for nitride VCSELs	36
3.6	Theoretical Analysis on Potential and Electrical Conductivity of AlGaN/GaN DBRs	42
3.7	Summary	49
<b>Chapter 4</b>	<b>Development of Fabrication Processes for III-Nitride Vertical-Cavity Surface-Emitting Devices</b>	51
4.1	Introduction	51
4.2	Development of Hole Injection Method	53
4.2.1	Activation of Mg Acceptor in Mg-doped GaN by Rapid Thermal Annealing	53
4.2.2	Fabrication and Characterization of p-Contacts for III-Nitride Vertical-Cavity Surface-Emitting Devices	53
4.3	Development of Fabrication Processes especially suitable for III-Nitride Surface Emitting Devices	60
4.3.1	Photolithography Suitable for High Density Nitride Surface Emitting Devices	60
4.3.2	Substrate Preparation Method for Nitride Surface Emitting Devices with Thick, High Reflectivity DBRs	63
4.4	Summary	65
<b>Chapter 5</b>	<b>Fabrication and Characterization of InGaN Vertical Microcavity LEDs</b>	67
5.1	Introduction	67
5.2	Fabrication of InGaN Vertical Microcavity LEDs	68
5.3	Characterization of InGaN Vertical Microcavity LEDs	73
5.3.1	Optical Properties	73
5.3.2	Electrical Properties	77
5.4	Prospects for Nitride Vertical-Cavity Surface-Emitting Lasers	78
5.5	Summary	79

<b>Chapter 6</b>	<b>Development of Fabrication Processes for AlN Photonic Crystal Nanocavities</b>	81
6.1	Introduction	81
6.2	Design of AlN photonic crystals	82
6.3	Fabrication processes patterning fine structures	85
6.4	Photoelectrochemical etching of SiC substrate	89
6.5	Summary	96
<b>Chapter 7</b>	<b>Characterization of AlN Photonic Crystal Nanocavities with GaN Quantum Dots</b>	97
7.1	Introduction	97
7.2	Optical Characterization of AlN Photonic Crystal Nanocavities	98
7.2.1	Experimental Setup of Microscopic Photoluminescence Measurements	98
7.2.2	Results of Microscopic Photoluminescence Measurements	100
7.3	Discussions	106
7.4	Summary	109
<b>Chapter 8</b>	<b>Concluding Remarks</b>	111
8.1	Summary of This Research	111
8.2	Future Prospects	113
<b>References</b>		115
<b>Publication Lists</b>		129



# Chapter 1

## Introduction

### 1.1 Background and Main Object of This Research

III-nitride semiconductors, namely AlN, GaN, InN, and their alloy compounds, have various superior properties compared with other compound semiconductors: direct and large bandgaps, large exciton binding energies, chemical inertness, high thermal conductivities, and so on. Thus, III-nitride semiconductors have been expected as promising materials for short-wavelength optoelectronic device or high-mobility electronic device applications and been studied long since late 1960s <sup>[1]</sup>. Though initial efforts conducted by limited number of research groups had revealed fundamental properties of the materials, developments of practical devices had remained still far from maturity mainly due to their difficulties to grow high quality crystals. The most frequently used substrate for heteroepitaxial growth of GaN is *c*-plane  $\alpha$ -Al<sub>2</sub>O<sub>3</sub>, or sapphire, whose in-plane lattice constant *a* is still considerably different from that of GaN. Due to their large (~ 16 %) lattice mismatch, GaN films grown directly on *c*-plane sapphire substrates tend to have extremely dense network of defects. In 1986, Amano et al. introduced low-temperature deposited AlN buffer layer, by which sufficiently high quality single crystals can be obtained, in metalorganic chemical vapor deposition (MOCVD) heteroepitaxial growth of nitride semiconductors <sup>[2]</sup>. Furthermore, they also developed an acceptor activation technique utilizing low energy electron beam and realized p-type conductivity in Mg-doped GaN and first p-n junction device in 1989 <sup>[3]</sup>. In 1991, Nakamura et al. developed so-called “two-flow MOCVD” growth technique and succeeded to establish a practical method to get p-type conductivity in Mg-doped GaN <sup>[4]</sup>. This achievement finally led to the world’s first, commercial nitride blue/violet light emitting diodes (LEDs) (1993), and laser diodes (1996) <sup>[5]</sup>.

There are various applications in which short-wavelength optical devices are potentially used: for example display devices, printing systems, optical data storages, medical apparatus, high

resolution measurement systems, lighting, and so on. Owing to their brightness and availability of nearly ideal purity of colors, LEDs make it possible to display high-fidelity full-color images. It is also expected that fluorescent tubes will be partly replaced by solid-state white LEDs when their efficiencies over 100 lm/W. On the other hand, nitride-based blue laser diodes are now used for the light source of optical pickups in high-density optical data storage systems such as blu-ray discs (BD) or high-density DVD (HD-DVD). Smaller size of beam spots, in other words higher density of recorded pits, is achieved with the blue lasers because the shorter wavelength is, the narrower beam waist can be obtained when a laser is focused by a lens.

However, further improvement of nitride blue light emitting devices are needed for various applications. For example, considering that parallel processing of an optical data storage system will offer faster read / write speed, a laser array integrated on a chip is favorable for such applications. Or, highly directional beam without any additional assembly such as epoxy mold is preferable to couple external optics.

Vertical microcavity LEDs (MCLEDs), in which an optical cavity with thickness on the order of the wavelength is sandwiched by planar cavity mirrors, have advantages such as improved spectral purity or improved directionality, which provide higher efficiency of the light emitting devices <sup>[6]</sup>. In addition, such devices are small in volume, which enables single mode operation with large modulation bandwidth <sup>[7]</sup>. Since emission wavelength in the microcavity LEDs is determined by the cavity resonance which directly reflects the structural parameters of the cavity, temperature stability of the emission wavelength is better in the devices than in conventional LEDs <sup>[8]</sup>. MCLEDs are attractive for those advantages which can expand the limitations of present LEDs <sup>[9,10]</sup>, and can meet the demand for high-performance LEDs.

Vertical-cavity surface-emitting lasers (VCSELs) and MCLEDs have similar structures, except that very high reflectivity is required for the cavity mirrors in VCSELs. VCSELs were first proposed by Iga in 1977 <sup>[11]</sup>, and have been investigated extensively in many research groups all over the world. Semiconductor vertical cavity sandwiched by two distributed Bragg reflectors (DBRs) provides very small volume of active region compared to edge-emitting lasers, hence various superior characteristics such as lower threshold current density, higher modulation frequency, or better temperature stability are theoretically expected and experimentally demonstrated <sup>[11]</sup>. If nitride edge-emitting lasers are replaced by nitride VCSELs, mode patterns, directionality and also above-mentioned characteristics (threshold current density, modulation frequency, and temperature

stability) are expected to be improved. For optical data storage applications, two-dimensionally integrated nitride VCSEL array enabled parallel processing to high-density optical disks and high speed read / write will be achieved with such devices <sup>[12]</sup>. Similar approach using VCSEL array to increase data transfer rate in optical data storage system has been proposed by Goto et al <sup>[13]</sup>.

Until now, there is no scientific report on electrically-driven lasing operation of nitride VCSEL in spite of continuous research efforts worldwide<sup>1</sup>. Based on their achievements to grow high quality AlGaIn/GaN DBRs by MOCVD <sup>[14]</sup>, Someya et al. demonstrated optically-pumped operation of nitride VCSEL at 77K <sup>[15]</sup> and at room temperature <sup>[16]</sup>. Other groups also reported optically-pumped lasing of nitride VCSELS <sup>[17-23]</sup>. One of the most difficult problems to realize the current-injection operation of nitride VCSEL is to obtain high-quality, electrically conductive nitride DBRs.

One of the main subjects of this research is to demonstrate high-performance III-nitride LEDs incorporating electrically-conductive nitride DBRs, which eventually contribute to establish fundamental technologies to realize electrically-driven nitride VCSELS.

On the other hand, quantum information technologies, within which quantum computing as well as quantum cryptography is included, are attracting much more interests nowadays. Quantum cryptography is regarded as an alternative of contemporary cryptography schemes used in modern telecommunication systems. According to the quantum mechanical nature of single photon, eavesdropping can be perfectly detected by the communicators in the quantum cryptography based on proposed protocols such as BB84 <sup>[25]</sup>. Usually, experimental quantum cryptography systems have been utilizing weakened coherent light produced by lasers in spite of pure single photon queues. In such system, poissonian behavior of the light source results in unexpected possibilities of two- or multi-photons events as well as no-photon events. Hence one can establish more ideal system using pure single-photon emitters. Efforts for fabricating such single-photon emitters are now under way worldwide and various kinds of single-photon emitters are proposed, including nitrogen vacancy color centers in diamond <sup>[26]</sup>, molecules <sup>[27]</sup>, or single atoms in optical cavities <sup>[28]</sup>. Among them, semiconductor quantum dots are considered as most practical way to construct single-photon

---

<sup>1</sup> We have found a patent which describes current-injection operation of nitride VCSELS, applied by Toshiba <sup>[24]</sup>. In this patent, written in Japanese, the inventor insists that the nitride VCSEL they fabricated was operated at room temperature and continuous-wave (CW) condition, with threshold current of 5 mA, operation voltage of 3.1 V, and emission wavelength of 400 nm. Truth is confidential and we don't know whether they are facts or not. It is regretful there is no scientific literature published, to our best knowledge, written by them concerning such remarkable results.

emitting devices <sup>[29-31]</sup>.

Semiconductor quantum dots (QDs), sometimes referred as artificial atoms made by semiconductors, have fundamentally discrete density of states due to their 3-dimensional confinement <sup>[32]</sup>. Carriers injected into the quantum dots might recombine at the unique energies, exhibiting delta-function like spectrum in the frequency domain. With these specific natures, quantum dots have been expected to be useful for many attractive applications including lasers, optical amplifiers, detectors, and single-photon emitters. For example, fast carrier dynamics can lead to very high frequency operation of the QD lasers. In III-nitride semiconductors, threshold current density of quantum well (QW) lasers are inherently higher than other III-V materials because of their relatively large electron effective masses. The threshold current density  $J_{th}$  of III-nitride QW lasers are  $\sim 10^3$  A/cm<sup>2</sup>, about one order of magnitude higher than that of GaAs-based QW lasers. When QDs with sufficiently small size are used in the active region, the threshold current of both III-nitride and GaAs-based lasers is almost the same. Hence the threshold current density reduction effect is more prominent in III-nitrides <sup>[33,34]</sup>.

There have been several reports on III-V semiconductor QD based single-photon emitters, both optically-pumped <sup>[30]</sup> and electrically-driven <sup>[35]</sup>. In such III-V single-photon emitters, however, there are limitations in terms of available wavelength, efficiency, or operation temperature. One can expect that more temperature-insensitive single-photon emitters are available when III-nitride semiconductors, in which exciton binding energies are greater than other III-V materials, are used. Kako et al. reported single photon generation up to 200 K <sup>[36]</sup>. Also, short wavelength emitted from nitride semiconductors can be useful to implement single-photon emitters in the satellite-based quantum communication systems. Because diffraction losses severely limit the total efficiency of such long-distance telecommunication systems, shorter wavelength is more preferable. Atmospheric turbulence has crucial influences only for the ground-based transmitter configuration with short wavelength photons <sup>[37]</sup>. Therefore, short wavelength single photon sources can be useful for satellite-to-satellite communication.

The efficiency of the single-photon emitters can be improved by introducing photonic crystals. Photonic band gap (PBG) materials, or photonic crystal in which refractive indices of constituent materials are periodically modulated and hence photon density of states is modified were predicted by Yablonovitch et al. in 1987 <sup>[38]</sup>. It can be described as an analogy of electron confinement systems in a periodic potential exhibiting inhibited energy bands. Although complete photonic band gap can

only be obtained by 3-dimensional (3D) photonic crystal, planar cavity consists of Bragg reflectors and 2-dimensional (2D) photonic crystal slab can be considered as a 1-dimensional (1D) and a 2D PBG material, respectively. With 2D photonic crystals, one can manipulate photons inside the nanocavity in more sophisticated way. Purcell spontaneous emission enhancement factor  $F$  is given as follows <sup>[39]</sup>:

$$F = \frac{3Q\lambda^3 \varepsilon_0}{4\pi^2 V n^3 \varepsilon_M}, \quad (1.1)$$

where  $Q$  means the quality factor of the cavity,  $V$ ,  $\lambda$ ,  $\varepsilon_0$ ,  $\varepsilon_M$ ,  $n$  mean the cavity mode volume, the wavelength of light, the dielectric constants of free-space and the location of exciton, respectively. Since one can reduce the mode volume of the cavity to the order of  $(\lambda/n)^3$  and can obtain high  $Q$ -factor in the order of tens or even hundreds of thousands in 2D photonic crystal slab, very large  $F$  is theoretically predicted in such structures. It is also expected that the extraction efficiency can be greatly improved by employing 2D photonic crystal slab in which in-plane guided modes are prohibited to exist and emitted power is effectively coupled to the radiation modes <sup>[40, 41]</sup>. With these two effects, the efficiency of a semiconductor quantum dot single-photon emitter can be dramatically improved.

As described above, nitride photonic crystal nanocavities with embedded quantum dots are highly promising for high-efficiency, high-temperature single-photon emitters. However, there are several issues to be overcome to fabricate such nanocavities: fine structure, removal of the substrate. The other target of this research is to develop fundamental technologies for fabrication of nitride-based photonic crystal nanocavities with quantum dots.

Now, let us summarize the major objects of this thesis. Among various possible nanostructures combining III-nitride semiconductors and nanocavities, the author will present, in this thesis, the developments on electronically-driven nitride vertical-microcavity LEDs and nitride photonic crystal nanocavities with embedded nitride quantum dots.

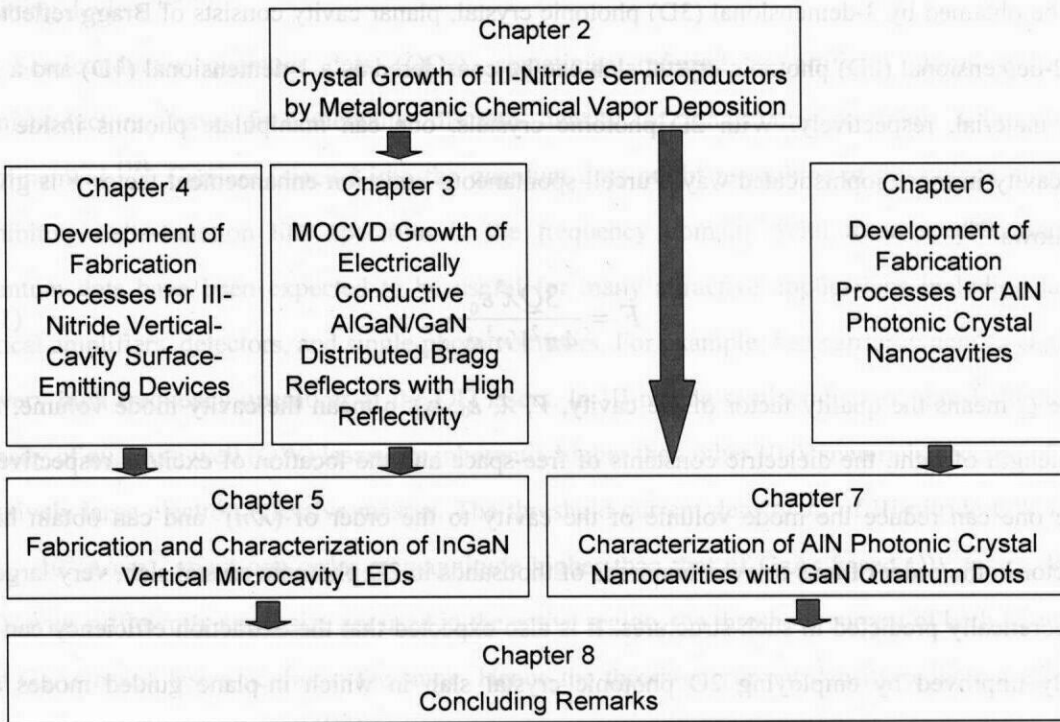


Figure 1.1 Construction of the thesis

## 1.2 Outline of This Thesis

In this thesis, the author describes the experimental results on fabricating nitride semiconductor micro- and nanocavity light emitters, namely InGaIn vertical microcavity LEDs and AlN photonic crystal nanocavity with GaN quantum dots. Figure 1.1 shows the relations between each chapters.

In Chapter 2, Basic principles of crystal growth of III-nitride semiconductors by metalorganic chemical vapor deposition (MOCVD) are presented. Details on experimental setups for the growth as well as fundamentals on MOCVD growth of nitride quantum dots are also given. Special efforts are made to improve crystal quality of thin AlN layers requisite to construct photonic crystal slab structure. Alternate supply of source gases is revealed to be effective to control surface morphology and relaxation process in the initial stage of AlN epitaxial growth. Utilizing that, thin AlN layer with sufficient quality is able to be grown. GaN QDs are grown on the thin AlN layer and characterized.

Chapters 3, 4, and 5 describe growth, fabrication, and characterization of InGaIn microcavity LEDs, respectively. In Chapter 3, MOCVD growth of electrically conductive AlGaIn/GaN DBRs is discussed. Structural, optical and electrical properties of the DBRs are studied systematically. From Si doping concentration dependence of structural and optical properties of n-DBRs, it can be

concluded that reasonable reflectivity can be maintained with uniform carrier concentration profile of  $1 \times 10^{18} \text{ cm}^{-3}$ . The author shows that the carrier concentration in n-AlGaIn layers can be increased up to  $3 \times 10^{18} \text{ cm}^{-3}$  while that of n-GaN is kept at constant value,  $1 \times 10^{18} \text{ cm}^{-3}$ , without further degradation of optical properties. Using such modulated doping profiles, electrical properties of the n-DBRs can be improved. As a result, it is possible to obtain near 99 % reflectivity in electrically conductive n-type nitride DBRs. Further improvement in both structural and electrical characteristics can be achieved by introducing n-AlGaIn/n-GaN short-period superlattice into the n-DBRs. Theoretical analysis is performed to shed light on the physical origin of electrical conductivity in nitride n-DBRs.

Developments of fabrication processes for nitride vertical microcavity light emitting devices are presented in Chapter 4. The developed processes range from substrate preparation method for DBR growth to formation of transparent intracavity contact. Because at least one of cavity mirrors is made by insulating materials in practical device structures, it is reasonable to utilize transparent intracavity contact to overcome design issues concerning efficient hole current injection. For this purpose, indium tin oxide (ITO) is used in this study. Rapid thermal annealing of sputtered ITO films under nitrogen ambient can improve both electrical and optical properties of the films. To improve process yield in photolithographic liftoff, new double-layer resist technique is developed. Undercut resist profile favorable for liftoff as well as good adhesion onto nitride (and ITO) surface is available with this new method. Substrate preparation method to prevent thick AlGaIn/GaN DBR to crack is also established.

In Chapter 5, the author describes fabrication and characterization of InGaIn vertical microcavity LEDs. Magnetron-sputtered, transparent ITO film is employed as a p-contact. After the LED mesas is defined by  $\text{Cl}_2$ -based plasma etching, a 10.5 pairs of  $\text{SiO}_2/\text{ZrO}_2$  top mirror is evaporated and wet-etched, followed by formation of an Al n-contact. EL spectra of these LEDs have reduced linewidth, exhibiting clear effects of microcavity. The angle dependence of EL reveals blue shift of main mode due to DBR resonance. Furthermore, directionality of the microcavity LED is dramatically improved to half angle of around 10 degree, compared to that of conventional one. The results are promising for developing blue/ultraviolet VCSELs and high performance LEDs, as well as electrically-pumped single photon emitters.

Chapters 6 and 7 describe fabrication and characterization of AlN photonic crystal nanocavities, respectively. Developments of fabrication processes for AlN photonic crystal nanocavities are

described in Chapter 6. Preliminary calculations reveal technological requirements for the fabrication of AlN photonic crystal nanocavities. In addition to the requirement for fine patterns as small as 150-nm-period, the substrate must be removed in order to obtain sufficient optical confinement in the nanocavities. To this end, photoelectrochemical etching is employed to fabricate AlN photonic crystal nanocavities. Due to accumulated photogenerated holes, lateral etching of 6H-SiC substrate occurs just below the AlN/SiC interface, and partial lift-off of AlN epitaxial layer results in a convex-shaped air-bridge structure.

In Chapter 7, experimental results are given on optical characterization of AlN photonic crystal nanocavities with GaN quantum dots. Microscopic photoluminescence measurements are performed to investigate the optical properties of the nanocavities. For the lowest-order cavity mode of a 150-nm-period nanocavity with seven missing holes, luminescence linewidth of 0.16 nm corresponding to the Q-factor of more than 2,400, which is the highest Q for nitride-based PC nanocavities ever reported, was obtained. Discussions on the results including theoretical analysis are also presented.

In Chapter 8, summary of this thesis is presented. Future prospects of this research is also given.

# Chapter 2

## Crystal Growth of III-Nitride

## Semiconductors by Metalorganic

## Chemical Vapor Deposition

### 2.1 Introduction

III-nitride semiconductors have been grown by various methods. Almost four decades ago, GaN crystal growth was achieved by sublimation method <sup>[42]</sup>. After that, several growth methods such as high pressure high temperature process <sup>[43]</sup>, liquid phase epitaxy (LPE) <sup>[44]</sup>, and hydride vapor phase epitaxy (HVPE) <sup>[45]</sup> had been applied to obtain nitride crystals. Since Akasaki et al. developed so-called low-temperature AlN buffer growth and succeeded the first fabrication of III-nitride p-n junction <sup>[3]</sup>, the most popular method to grow nitride semiconductors is metalorganic chemical vapor deposition (MOCVD) or metalorganic vapor phase epitaxy (MOVPE) <sup>[46]</sup>. Although technological progresses in III-nitride growth include other methods such as molecular beam epitaxy (MBE) <sup>[47]</sup>, or pulsed laser deposition <sup>[48]</sup>, generally MOCVD has advantages in terms of uniformity, mass-productivity, and controllability of alloy composition. As for III-nitrides, superior quality of epitaxial films is readily available by using MOCVD and almost all commercial III-nitride semiconductor devices are now grown by the method <sup>[5]</sup>. The samples described in this thesis are all grown by MOCVD. Optimal growth conditions are required to obtain good crystalline quality. In particular, the growth of self-assembled quantum dots by Stranski-Krastanov growth mode is especially sensitive to the growth conditions, hence one must carefully optimize the conditions <sup>[49,50]</sup>. In this chapter, basic principles of crystal growth of III-nitride semiconductors by metalorganic chemical vapor deposition (MOCVD) are presented. Details on our experimental setups for the

growth as well as some specific conditions on MOCVD growth of nitride quantum dots are also given. Special efforts are made to improve crystal quality of thin AlN layers requisite to construct photonic crystal slab structure. Alternate supply of source gases is revealed to be effective to control surface morphology and relaxation process in the initial stage of AlN epitaxial growth. Utilizing that, thin AlN layer with sufficient quality is able to be grown. GaN QDs are grown on the thin AlN layer and characterized.

## 2.2 Principles of Crystal Growth of III-Nitride Semiconductors by Metalorganic Chemical Vapor Deposition

MOCVD or MOVPE (metalorganic vapor phase epitaxy) has been widely used as a standard growth method for III-V compound semiconductors. Since there is almost no substrate lattice-matched to the nitride semiconductor, in most cases sapphire ( $\alpha\text{-Al}_2\text{O}_3$ ) (0001) or 6H-SiC (0001) have been used as substrates for the heteroepitaxial growth of III-nitrides. Various alternative materials such as GaAs<sup>[51]</sup>, Si(111)<sup>[52]</sup>, and ZrB<sub>2</sub> have been also used as the substrate<sup>[53]</sup>. Recently, several factories have developed GaN substrates obtained by various growth techniques and they are now commercially available<sup>[54,55]</sup>. Although GaN substrates are ideal for most GaN-based devices, excellent quality substrate is still very expensive. Instead, sapphire substrates are easily available and widely used to grow high-quality nitride crystals with so-called epitaxial lateral overgrowth method<sup>[56]</sup>.

In Figure 2.1, a schematic illustration of the MOCVD equipment used in this study is shown. The system, a custom-made horizontal reactor manufactured by Nippon-Sanso (Taiyo Nippon Sanso co. ltd. at present), was rebuilt to grow III-nitrides in 1997, whereas it had originally been used to grow GaAs-based materials. In MOCVD of III-V semiconductors, group-III metalorganic precursors are introduced with carrier gases into growth chamber where substrates are located on susceptors and heated. In this study, nitrogen and hydrogen are usually used as the carrier gases. Hydrogen is purified by using a platinum-palladium membrane filter. Group III materials (Al, Ga, In) are supplied as their alkyl compounds: for example trimethylaluminum (TMA) for Al and trimethylgallium (TMG) for Ga. The precursors are contained in stainless-steel bottles or cylinders and set at appropriate temperatures in order to get sufficient equilibrium vapor pressures. In this experiment, the temperatures of precursors are kept at 20.0 °C, -4.2°C, 47.2°C, and 25.0°C for TMA, TMG, trimethylindium (TMI), and a p-type dopant, bis-cyclopentadienyl-magnesium (Cp<sub>2</sub>Mg),

respectively. The pressure inside the cylinders for all of the precursors except TMI was maintained at 950 Torr, while that of TMI was kept at 850 Torr. Ultra-pure  $\text{NH}_3$  is supplied as the source of nitrogen. Also, monosilane ( $\text{SiH}_4$ ) diluted in  $\text{H}_2$  at concentration of 10 ppm is used as an n-type dopant.

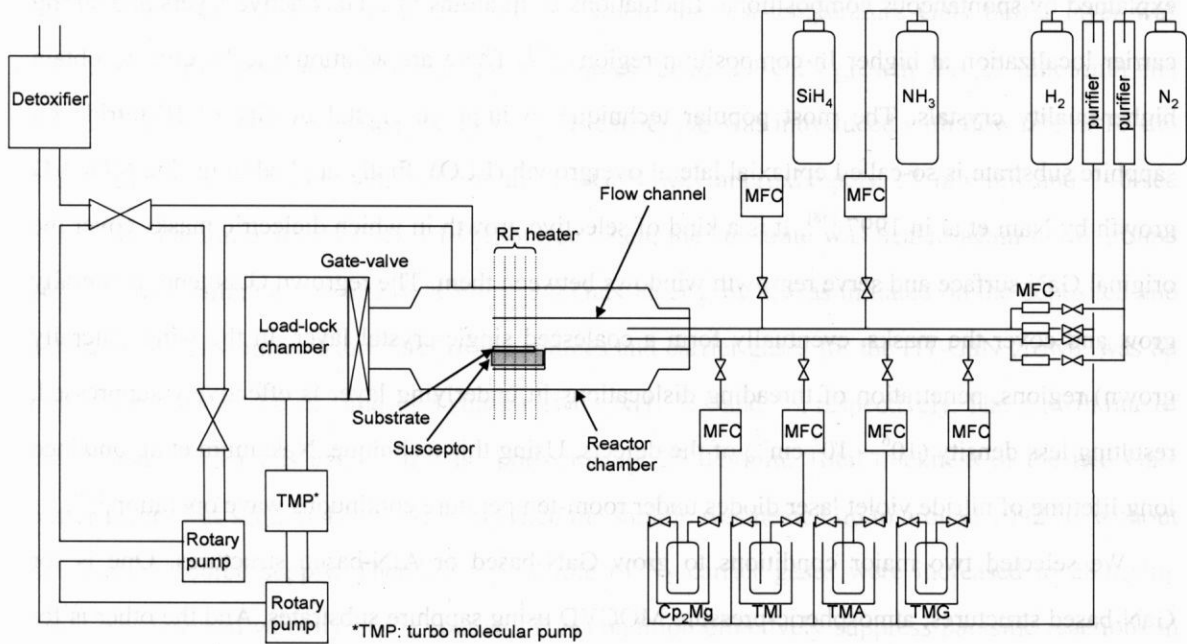


Figure 2.1 Schematic illustration of the MOCVD system

In most cases of heteroepitaxial growth of GaN on sapphire by MOCVD, so-called two-step growth or low-temperature buffer growth method is applied to overcome lattice mismatch and thermal expansion coefficient difference <sup>[2,4]</sup>. In this technique, an amorphous or polycrystalline AlN or GaN is first deposited on the substrate at relatively low temperature (~ 500 °C). During heating up to the growth temperature around 1100 °C, the buffer layer is crystallized and allows one to grow single-crystalline GaN layer on it. Normally, the MOCVD-grown GaN single crystal epitaxial layer has very high density ( $10^8 \sim 10^{11} \text{ cm}^{-2}$ ) of threading dislocations. Despite the enormous density of defects, light emitting diodes fabricated with such crystal yet exhibit high efficiency <sup>[5]</sup>. It can be explained by spontaneous compositional fluctuations of In atoms in InGaN active layers and strong carrier localization at higher In composition regions <sup>[57]</sup>. There are additional techniques to obtain higher-quality crystals. The most popular technique to improve crystal quality of III-nitride on sapphire substrate is so-called epitaxial lateral overgrowth (ELO), firstly applied in nitride MOCVD growth by Nam et al in 1997 <sup>[58]</sup>. It is a kind of selective growth in which dielectric masks cover the original GaN surface and serve regrowth windows between them. The regrown GaN tend to laterally grow and cover the masks, eventually form a coalesced single-crystal layer. In the wing (laterally grown) regions, penetration of threading dislocations in underlying layer is effectively suppressed, resulting less density ( $10^6 \sim 10^7 \text{ cm}^{-2}$ ) of the defects. Using this technique, Nakamura et al. obtained long lifetime of nitride violet laser diodes under room-temperature continuous wave operation <sup>[59]</sup>.

We selected two major conditions to grow GaN-based or AlN-based structures. One is for GaN-based structures: atmospheric-pressure MOCVD using sapphire substrates. And the other is for AlN-based ones: low-pressure MOCVD using 6H-SiC substrates. These two sets were used exclusively because higher quality GaN can be obtained by the atmospheric-pressure condition and higher quality AlN can be obtained by the low-pressure condition. For the atmospheric-pressure growth, substrates used were commercially available c-face sapphire supplied by Kyocera. Dimensions of the substrate is 21 mm × 16 mm × 0.33 mm. For the low-pressure growth, we used n-type 6H-SiC(0001) substrates supplied by CREE inc. Original 2" substrate was cleaved into typically 6 mm × 6 mm in size. The substrate was set on a graphite susceptor coated with SiC. In order to suppress turbulence and to obtain homogenous epilayers near the substrate edges, dummy substrates were located surrounding the substrate.

## 2.3 General Growth Conditions for III-Nitride Vertical Microcavity Light Emitting Devices

In Figure 2.2, a diagram showing growth conditions for the GaN/AlGaIn distributed Bragg reflector which is a key structure of vertical microcavity light emitting devices is presented. The devices were all grown onto sapphire substrates at atmospheric-pressure.

At first, the substrate was heated up to 930 °C at the ramping rate of 150 °C/min and then was hold at the temperature for 4 min under constant NH<sub>3</sub> flow of 0.5 slm (standard litter per minutes). During this stage, surface of the sapphire substrate was cleaned and nitridated. After the cleaning, the substrate was cooled down to around 480 °C, where the low-temperature GaN buffer layer was deposited on the substrate. Flow rates of the sources for the LT-GaN growth was 22 μmol/min and 3.5 slm for TMG and NH<sub>3</sub>, respectively. Only H<sub>2</sub> carrier gas was introduced with flow rate of 16 slm during the growth. The growth rate of the LT-GaN was approximately 17 nm/min and 140-sec growth resulted in a 40-nm-thick LT-GaN layer. Then, the substrate was heated again up to around 1071 °C with ramping rate of 210 °C/min, and GaN layer growth was initiated on the deposited and annealed LT-GaN buffer. Flow rates of the sources and carrier gases for the HT-GaN growth was 88 μmol/min, 4.0 slm, 4.0 slm and 11.5 slm for TMG, NH<sub>3</sub>, H<sub>2</sub>, and N<sub>2</sub>, respectively. The growth rate of the HT-GaN under this condition was approximately 25 nm/min. Total thickness of the two GaN buffer layers was set at  $5/4\lambda$  (~192 nm). Then the sample was heated up to around 1092 °C without interrupting source supply. Thereafter, flow rate of N<sub>2</sub> carrier gases were increased to 28.0 slm, resulting increased velocity of the sources. This condition effectively suppress parasitic reactions in the gas phases between NH<sub>3</sub> and TMA. Quarter-wavelength AlGaIn and GaN layers were stacked on the GaN buffer. Al<sub>x</sub>Ga<sub>1-x</sub>N layers were grown with various TMA flow rates in order to control Al composition x. Typically, using TMA and TMG flow rates of 27 μmol/min and 16 μmol/min with 4.0 slm NH<sub>3</sub> flow, approximately 40 % Al composition can be obtained. Growth rate of GaN with total carrier flow rate of 32.0 slm was decreased to 15 nm/min. Growth rate of the AlGaIn layer was 3.8 nm/min with above-mentioned conditions. When the whole structure was grown, supply of the metalorganics were halted and RF heater was off. NH<sub>3</sub> flow was stopped after the substrate was cooled below 500 °C. The sample was brought out from the reactor after cooling and evaluated optically or structurally.

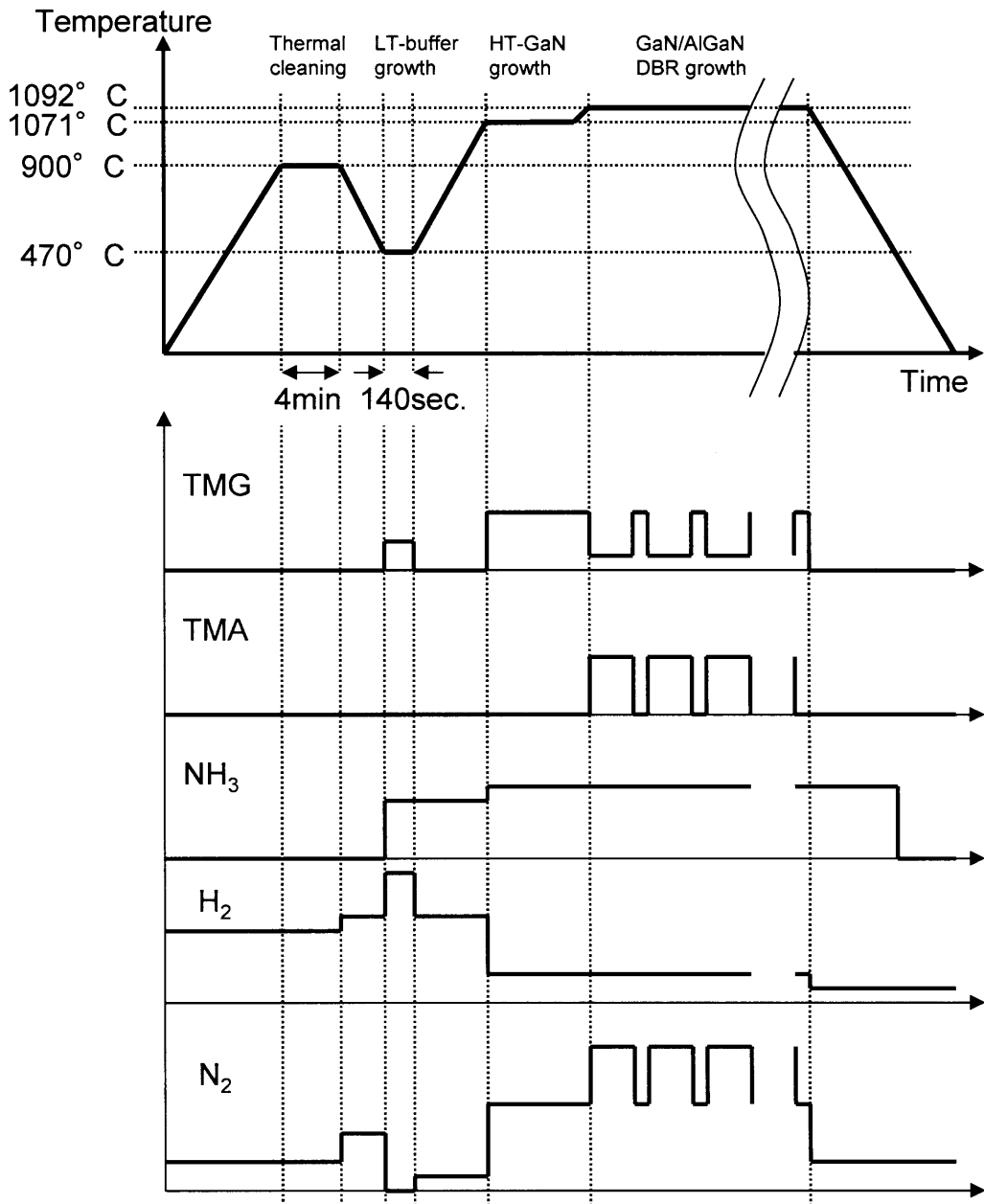


Figure 2.2 Schematic diagram of growth sequence for GaN/AlGaN DBRs

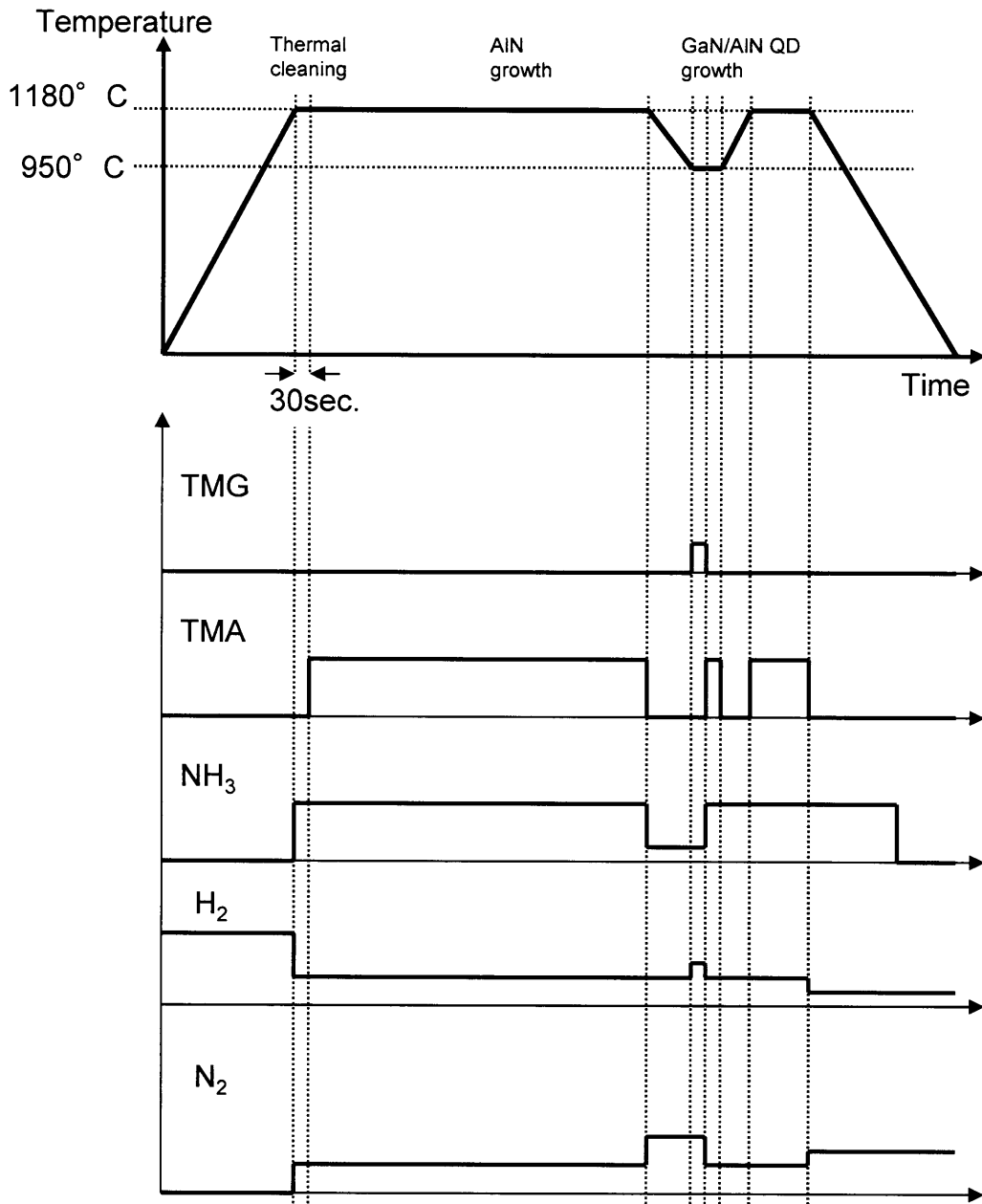


Figure 2.3 Schematic diagram of growth sequence for GaN/AlN QDs

## 2.4 General Growth Conditions for GaN/AlN Quantum Dots

As described in the previous chapter, semiconductor quantum dots are attractive from the viewpoint of not only fundamental quantum physics but also device applications. To fabricate such three-dimensional, nanometer-scale structures have been one of the hottest topics in solid-state electronics. Recent technological progress in nanofabrication allows one to successfully fabricate such nanostructures. From practical aspect, epitaxially grown semiconductor QDs are one of the most promising technologies among various developments. In general, heteroepitaxial growths are classified into three schemes; layer-by-layer or two-dimensional growth, island or three-dimensional growth, and intermediate or two-to-three evolutionary growth. The two-dimensional growth mode is referred as Frank-van der Merwe (FdM) growth mode, while the three-dimensional one is called Volmer-Weber (V-W) mode. The intermediate mode, or so-called Stranski-Krastanov growth mode is characterized by initial two-dimensional growth and following three-dimensional growth due to the accumulated compressive strain inside the epitaxial layer. Using the S-K growth mode, III-V or II-VI QDs have been successfully fabricated. Nowadays, infrared lasers or semiconductor optical amplifiers (SOAs) in which InAs-based QDs are embedded are close to be commercially available [74].

Our group have been developed the S-K growth of GaN/AlN QDs by MOCVD [49]. Generally, GaN quantum dots (QDs) can be formed on AlN with extremely low V/III ratio. Standard V/III ratio to grow GaN layers is in the order of 10,000, whereas the optimized V/III ratio for the GaN QD growth is three order of magnitude lower than that,  $\sim 10$ . Such a low V/III ratio is effective to suppress the surface migration of Ga adatoms and crucible to obtain high-quality high-density nanometer-size dots. Growth temperature is another deterministic factor for the GaN QD formation. At higher temperature and under sufficient supply of  $\text{NH}_3$ , GaN tend to grow two-dimensionally. On the contrary, At lower temperature and under lower V/III ratio, migration of Ga adatoms is suppressed, eventually causes three-dimensional growth with forming giant hillocks. Formation of GaN QD seems to occur under intermediate conditions between the above-mentioned two situations. Density or size of the QDs are quite sensitive to the growth conditions. Especially, since the optimum temperature ranges only within approximately 20 K window, one must precisely control the growth temperature with high accuracy.

GaN/AlN quantum dot samples were grown by low-pressure metalorganic chemical vapor deposition system. Figure 2.3 shows schematic diagrams for growth of GaN/AlN QDs. The growth

pressure was set to 200 Torr throughout the growth. At first, a 100-nm-thick AlN layer was grown on n-type 6H-SiC (0001) substrates at 1180 °C without any buffer layer. Self-assembled GaN quantum dots were then grown in Stranski-Krastanov mode on the AlN at around 960 °C, followed by the two-step growth of an AlN capping layer: firstly a 4-nm-thick layer at the quantum-dot growth temperature and secondly a 16-nm-thick layer at 1180 °C. A reference sample without capping layer was prepared with the same conditions to investigate surface morphology of the GaN quantum dots. Figure 2.4 shows an atomic force microscope image of the reference sample. Density, average height and diameter of the dots were  $2.3 \times 10^{10} \text{ cm}^{-2}$ , 4.6 nm, and 29 nm, respectively.

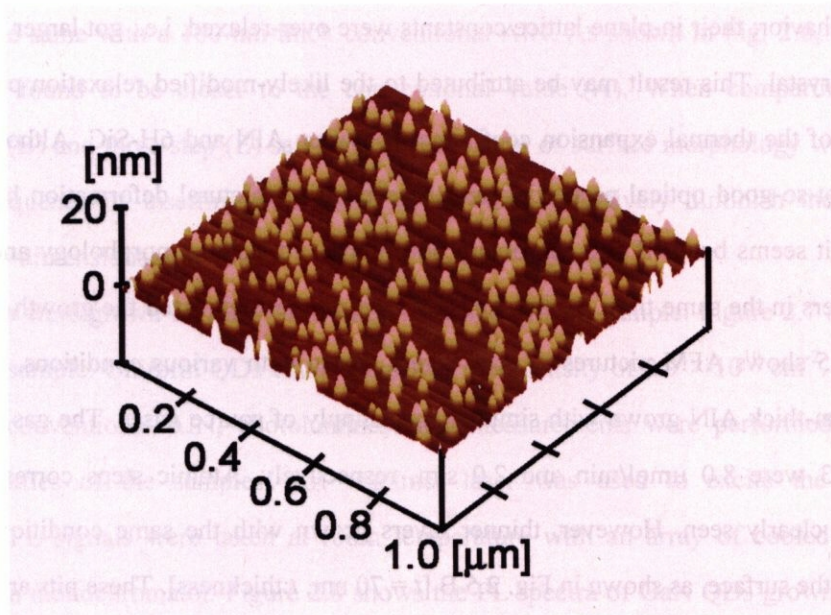


Figure 2.4 AFM image of standard GaN/AlN quantum dots

In order to obtain lower defect density in epitaxial AlN layer, the new growth conditions have been developed. Since defect states are considered to be responsible to the spectral diffusion in GaN QDs [61], it is very important to suppress unfavorable effect from defects and to grow higher quality AlN matrix. When AlN-based photonic crystal nanocavities with embedded GaN QDs are considered, very thin layer is required for the slab structure to achieve a large Q-factor. Recently, we have found that the alternate supply of TMA and NH<sub>3</sub> can improve surface morphology of AlN layers [62]. That is attributed to the suppressed gas-phase parasitic reactions. Atomic force microscope observation revealed that the alternate-supply grown AlN had lower density of large pits and had flatter surface without spiral growth than conventional ones (grown with simultaneously supplied source gases). It seemed that the alternate supply method tend to enhance lateral growth and consequently larger domains appears even when the underlying layer consists rough island-like grains. However, the alternate-supply has disadvantages in terms of GaN QD formation above it. The optical properties of the GaN QDs directly grown on the alternate-supply AlN were not improved or even got worse. X-ray analysis revealed that the alternate-supply grown AlN exhibited an eccentric behavior; their in-plane lattice constants were over-relaxed, i.e., got larger than that of a free-standing crystal. This result may be attributed to the likely-modified relaxation process due to the difference of the thermal expansion coefficients between AlN and 6H-SiC. Although relations between the not-so-good optical properties and the eccentric structural deformation have not been perceived yet, it seems better if one can obtain both improved surface morphology and unchanged lattice parameters in the same time. To this end, we have further optimized the growth conditions of AlN. Figure 2.5 shows AFM pictures of AlN layers grown with various conditions. Figure 2.5 A shows a 100-nm-thick AlN grown with simultaneous supply of source gases. The gas flow rates of TMA and NH<sub>3</sub> were 8.0 μmol/min and 2.0 slm, respectively. Atomic steps corresponding one monolayer are clearly seen. However, thinner layers grown with the same conditions have high density pits on the surface, as shown in Fig. 2.5 B [ $t = 70$  nm,  $t$ :thickness]. These pits are presumably due to incomplete coalescence. On the other hand, a 80-nm-thick AlN grown thoroughly with alternate supply of TMA (1.5 sec) and NH<sub>3</sub> (1.5 sec) had very smooth feature, as shown in Fig. 2.5 C. In this growth, 1-second interruptions were inserted before and after the supply of each source gases. Flow rates of TMA and NH<sub>3</sub> were 8.0 μmol/min and 2.0 slm, respectively. N<sub>2</sub> with flow rate of 2.0 slm was introduced into the reactor when NH<sub>3</sub> was not flowed. An alternate gas for TMA was H<sub>2</sub>. Although the surface morphology was improved in terms of large-pit density, tiny (diameter ~ 5 nm)

pits were rather densely distributed on the surface. Furthermore, as described above, the in-plane lattice constant of the layer was strangely widened comparing to the bulk value. The in-plane (a-axis) and growth direction (c-axis) lattice constants of the AlN layers shown in Fig. 2.5 are plotted in Fig. 2.6. To investigate the growth-condition-dependent structural properties further, hybrid structures were grown. One was grown with two steps: firstly pulse-AlN and secondly conventional AlN, both with thickness of 35 nm (Fig. 2.5 D). And the other was grown with three steps: firstly conventional AlN (17.5 nm), secondly pulse-AlN (35 nm) and finally again conventional AlN (17.5 nm) (Fig. 2.5 E). The two-step growth (Fig. 2.5 D) exhibited intermediate surface morphology between conventional AlN (Fig. 2.5 B) and pulse-AlN (Fig. 2.5 C). However, the layer had still over-relaxed in-plane lattice constant as shown in Fig. 2.6. Suspecting the in-plane lattice constant was predominantly determined by what conditions were used for the relaxation process within the critical thickness of around 10 nm, the three-step growth was examined. In this case, conventional AlN was firstly deposited on the substrate up to 17.5 nm, above the critical thickness. Surface morphology was improved comparing to the two-step sample. The density of the monolayer steps was nearly the same with a 100-nm-thick conventional AlN. As shown in Fig. 2.6, in-plane lattice constant was found to be closer to the conventional value (A). When comparing 70-nm-thick conventional (B) and three-step (E) samples, improvement of surface morphology was outstanding. It is a consequence of inserting pulse-AlN layer, which effectively diminish the large pits by enhanced two-dimensional growth.

GaN QDs were grown on the 70-nm-thick modified growth sample. Figure 2.7 shows an AFM image of the sample. Uniform QDs could be grown with density of  $2.9 \times 10^{10} \text{ cm}^{-2}$ . Capped with a 50-nm-thick conventional AlN, photoluminescence measurements were performed to investigate optical properties of the samples. ArF excimer laser was used to excite the samples. The macroscopic PL signals were taken at room temperature with an array of cooled CCD detector connected to a monochromator. Figure 2.8 shows the PL spectra of GaN QDs grown with the same conditions on either conventional AlN (A) or modified AlN (B), both 70-nm-thick. Improvement on emission intensity was confirmed.

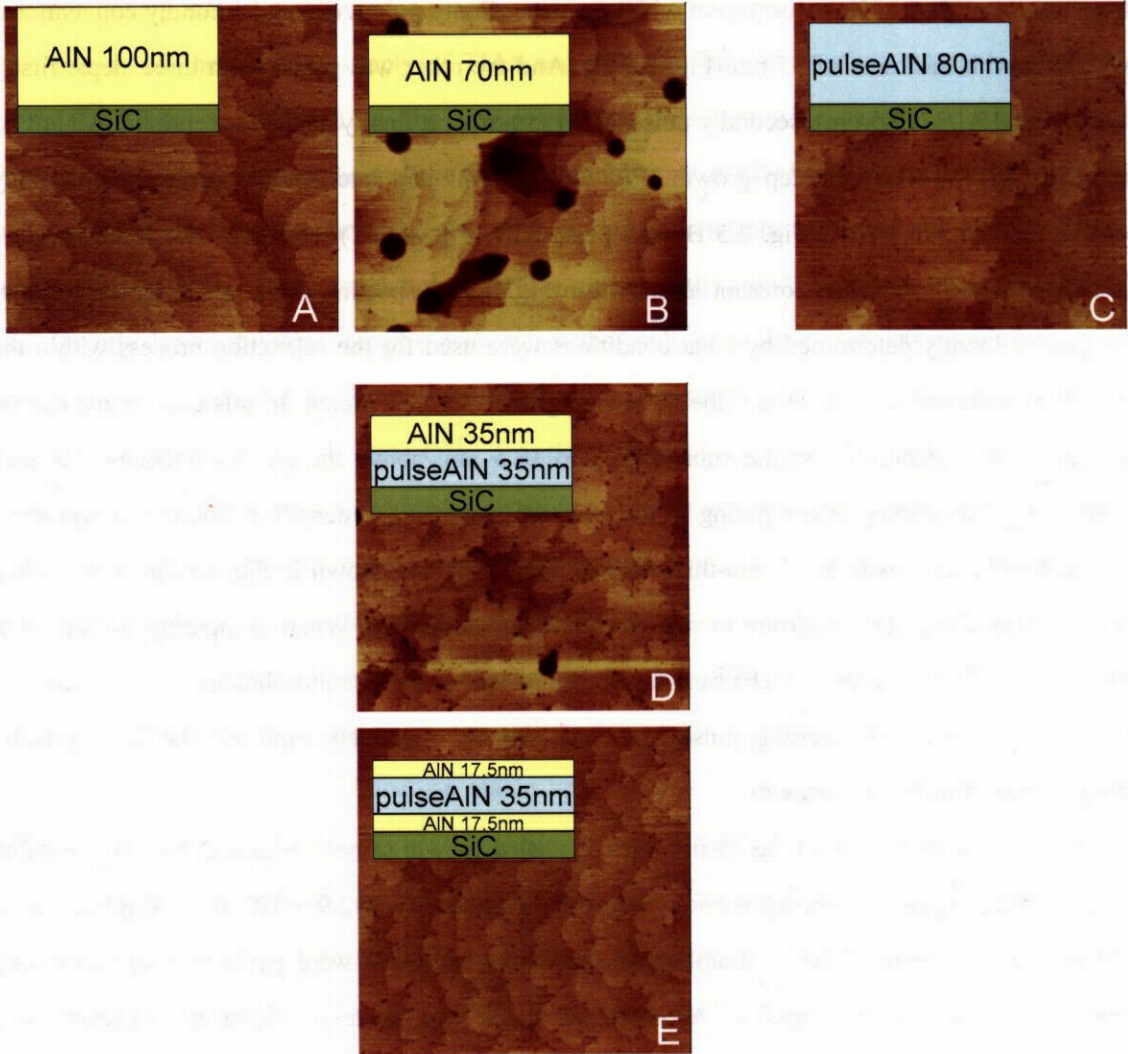


Figure 2.5 AFM images ( $1\mu\text{m} \times 1\mu\text{m}$ ) of AlN with various AlN growth conditions

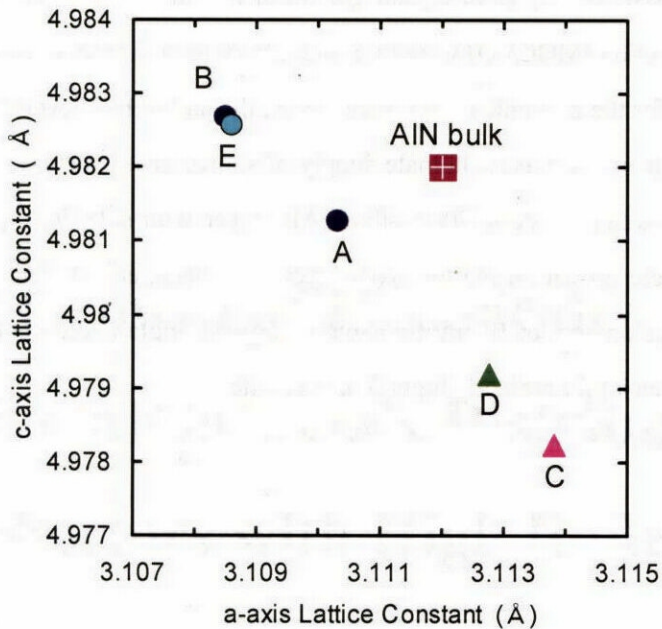
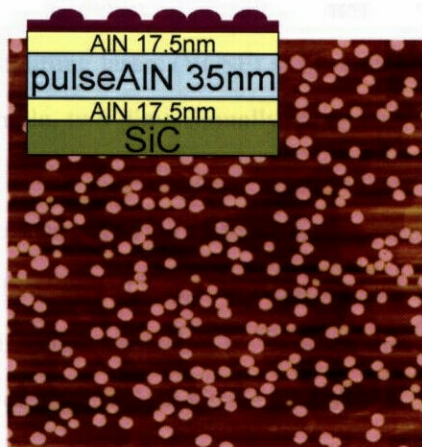


Figure 2.6 Lattice constants of AlN layers grown with various conditions



$2.9 \times 10^{10} \text{cm}^{-2}$   
 $\phi 23.4 \pm 4.7 \text{nm}$   
 $h 4.5 \pm 0.65 \text{nm}$

Figure 2.7 AFM images ( $1 \mu\text{m} \times 1 \mu\text{m}$ ) of GaN QDs grown on an optimized AlN

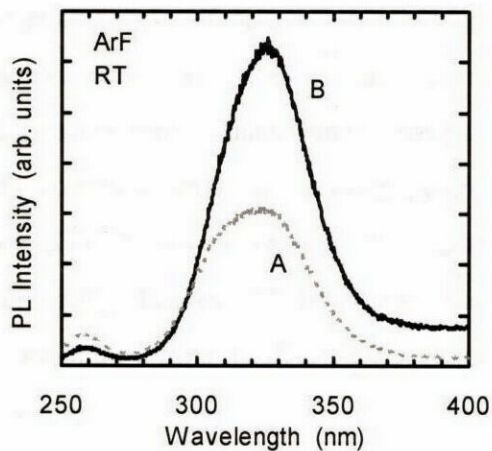


Figure 2.8 Room temperature PL spectra of capped GaN QDs grown on (a) a conventional 70-nm-thick AlN and (b) an optimized 70-nm-thick AlN

## 2.5 Summary

In this chapter, basic principles of crystal growth of III-nitride semiconductors by metalorganic chemical vapor deposition (MOCVD) were presented. In order to improve the crystal quality of thin AlN layers required for the photonic crystal nanocavity, the author has developed an optimal growth sequence of buffer layers, in which alternate supply of source gases was utilized to control surface morphology and relaxation process. 70-nm-thick AlN layer with sufficient quality was able to be grown. GaN QDs were grown on the thin AlN layer and characterized. This improvement is very important for the development of III-nitride photonic crystal single-photon emitters because thinner AlN buffer layer is crucial for realizing high-Q nanocavities.